

Porous Sr_2CuWO_6 Nanoarchitectures Fabricated by a Matrix-mediated Route

Xianluo Hu* and Jimmy C. Yu*

Department of Chemistry and Center of Novel Functional Molecules, The Chinese University of Hong Kong, Shatin, New Territories, Hong Kong, P. R. China

(Received October 17, 2008; CL-081000; E-mail: jimyu@cuhk.edu.hk)

A facile route based on a matrix-mediated process has been developed to fabricate porous double-perovskite oxide Sr_2CuWO_6 nanoarchitectures in large quantities.

Cuprate double-perovskite oxide, Sr_2CuWO_6 , is a known compound with a space group of $I4/m$ at room temperature.¹ It can be represented as a three-dimensional network of alternating CuO_6 and WO_6 octahedral units. Cu and W atoms exist in the center of the octahedra, while O atoms are on the vertices and Sr atoms occupy the interstitial spaces (Figures 1a and 1b). As a layered double perovskite, Sr_2CuWO_6 has been intensively investigated for its interesting structural and magnetic properties.^{2,3} As one of many challenges in the design and synthesis of nanomaterials, inorganic nanostructures with a distinctive geometrical shape and architecture have received increasing attention during the past decades because of their potential applications in catalysis, sensing, photonics, electronics, etc.^{4–11} Current methods to prepare bulk Sr_2CuWO_6 are mainly based on solid-state reactions.^{1–3} However, mass production of nanoarchitectured Sr_2CuWO_6 still remains a significant challenge to materials scientists and chemists.

Herein we report on a large-scale matrix-mediated (MM) method to prepare porous Sr_2CuWO_6 nanoarchitectures. Mainly, two steps were involved in the MM process. First, salt-containing precursor was formed based on a polymer matrix of sucrose (>98%, Aldrich) and poly(vinyl alcohol) (PVA, >98%, $M_r = 145000$, Aldrich). Then, the porous networks of Sr_2CuWO_6 were achieved by removal of the sacrificial matrix. In a typical procedure, $\text{Sr}(\text{NO}_3)_2$ (99.995%, 4 mmol), $\text{Cu}(\text{NO}_3)_2 \cdot 6\text{H}_2\text{O}$ (99.999%, 2 mmol), and $(\text{NH}_4)_2\text{WO}_4$ (99.99%, 2 mmol) were

dissolved in 20 mL of H_2O . Then, 3 g of PVA and 30 g of sucrose were added. The resulting mixture was stirred vigorously for 1 h at room temperature and subsequently heated at 80, 150, and 200 °C for 1 h, respectively. After that, a calcination process was carried out in static air at 900 °C (ramp rate at 5 °C min^{-1}) and held for 5 h to remove the polymer matrix and crystallize the inorganic framework. This resulted in green spongelike Sr_2CuWO_6 with continuous pore networks (yield: ca. 100%). In our approach, the polymer matrix of sucrose and PVA played a multifunctional role in the formation of porous Sr_2CuWO_6 nanostructures. Numerous hydroxy groups from the matrix could chelate with metal cations, leading to an atomic distribution of metal cations throughout the whole polymer network. Also, the polymer matrix could serve as an efficient internal fuel to decompose and burn out the precursor spontaneously into spongelike Sr_2CuWO_6 . Figure 1c shows a schematic illustration of the preparation process for the porous Sr_2CuWO_6 (Sample-MM). As a reference, microsized Sr_2CuWO_6 crystallites (Sample-SSR) were also prepared by a conventional solid-state reaction (SSR) route.^{1–3}

The crystallinity and phase of the Sr_2CuWO_6 products were characterized by powder X-ray diffraction (XRD, Bruker D8 Advance). Figure 2a displays a typical XRD pattern of the porous Sr_2CuWO_6 . The reflections can be readily indexed to tetragonal Sr_2CuWO_6 , in a good agreement with the literature values.¹² The XRD pattern of microsized Sr_2CuWO_6 crystallites is showed in Figure S1.¹³ The peak marked with an asterisk is possibly from SrWO_4 impurity, which is consistent with the literature results. Energy-dispersive X-ray (EDX) analyses were carried out to determine the chemical composition of the as-

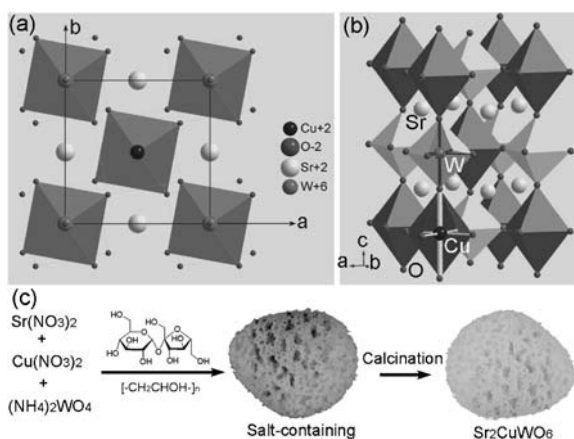


Figure 1. Crystal structure of Sr_2CuWO_6 with projection (a) along [001] and (b) perpendicular to [001]. (c) Schematic illustration of the preparation process for the porous Sr_2CuWO_6 nanoarchitecture.

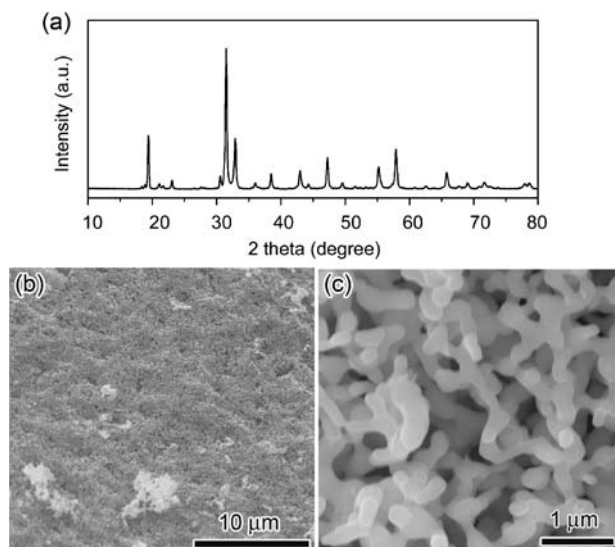


Figure 2. (a) XRD and (b, c) SEM images of Sample-MM.

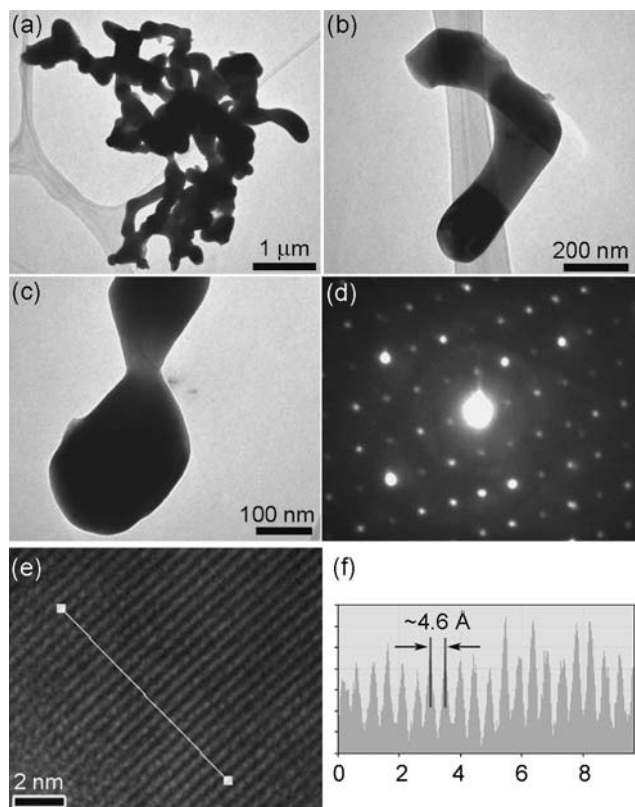


Figure 3. (a) Typical low-magnification TEM image of broken Sr_2CuWO_6 fragments. (b, c) High-magnification TEM images of individual broken ligaments. (d) SAED pattern. (e) HRTEM image taken at the edge of a single ligament. The periodic fringe spacing is highlighted with a line showing the lattice fringes of (101) planes of tetragonal Sr_2CuWO_6 . (f) Corresponding intensity profile for the line scan across the lattice fringes.

obtained samples (Figure S2). The EDX spectra confirm the presence of Sr, Cu, W, and O in both Sr_2CuWO_6 products.

Scanning electron microscopy (SEM, LEO, 1450VP) analyses were performed to examine the morphology of the samples. Figures 2b and 2c show the SEM images of Sample-MM. Apparently, it exhibits numerous well-defined macropores. Such a porous structure could be observed more clearly from SEM images recorded at a higher magnification. As shown in Figure 2c, Sample-MM consists of an interconnected framework of Sr_2CuWO_6 filaments, approximately 200 nm in width. The interconnecting filaments composed of rows and rings of fused nanoparticles enclose pores of 0.1 to 5 μm in size. Figures S3a and S3b show the SEM images for Sample-SSR. This sample exhibits the morphology of particle aggregates. The irregular crystallites have diameters ranging from 1 to 2 μm .

Transmission electron microscopy (TEM, CM-120, Philips, 120 kV) provided further insight into the morphological and

structural details of the porous Sr_2CuWO_6 . After ultrasonic irradiation, the broken MM- Sr_2CuWO_6 sample was dispersed on TEM copper grids. Figure 3a shows a representative TEM image for the broken fragments of Sr_2CuWO_6 filaments with diameters ranging from 80 to 200 nm. Figures 3b and 3c display the high-magnification TEM images of individual broken filaments. Foam-shaped Sr_2CuWO_6 is not a simple aggregation of small crystallites but is composed of interconnected single-crystalline ligaments that enclose numerous macropores. The selected area electron diffraction (SAED) pattern (Figure 3d) taken from a single ligament shows the single-crystal nature and can be indexed to the tetragonal Sr_2CuWO_6 , consistent with the XRD result. High-resolution TEM (HRTEM, Tecnai F20, FEI, 200 kV) images further confirm the single-crystal nature of the ligaments. Figure 3e shows a HRTEM image at the edge of an individual Sr_2CuWO_6 ligament. As shown in Figure 3f, a representative intensity profile covers the line scan (labeled by a line in Figure 3e) across the lattice fringes. The periodic fringe spacing of ca. 4.6 \AA corresponds to the interplanar spacing between the (101) planes of tetragonal Sr_2CuWO_6 .

The UV-vis reflectance spectra of the MM- and SSR- Sr_2CuWO_6 samples are shown in Figure S4. The band gap energies estimated from the onset of the absorption edge are 2.2 eV for Sample-MM and 2.3 eV for Sample-SSR.

In summary, porous double-perovskite oxide Sr_2CuWO_6 nanoarchitectures have been successfully fabricated using a matrix-mediated method. Our investigations show that the porous Sr_2CuWO_6 nanoarchitectures have a band gap of 2.2 eV. The resulting spongelike Sr_2CuWO_6 with continuous pore network and easy surface modification may be an ideal candidate as advanced catalytic supports and optic/electronic materials.

References and Notes

- 1 M. Gateshki, J. M. Igartua, *J. Phys.: Condens. Matter* **2003**, *15*, 6749.
- 2 M. W. Lufaso, W. R. Gemmill, S. J. Mugavero, Y. Lee, T. Vogt, H.-C. zur Loye, *J. Solid State Chem.* **2006**, *179*, 3556.
- 3 M. Gateshki, J. M. Igartua, E. Hernandez-Bocanegra, *J. Phys.: Condens. Matter* **2003**, *15*, 6199.
- 4 Y. Yin, A. P. Alivisatos, *Nature* **2005**, *437*, 664.
- 5 X. Wang, J. Zhuang, Q. Peng, Y. Li, *Nature* **2005**, *437*, 121.
- 6 Y. Sun, Y. Xia, *Science* **2002**, *298*, 2176.
- 7 J. Park, K. An, Y. Hwang, J.-G. Park, H.-J. Noh, J.-Y. Kim, J.-H. Park, N.-M. Hwang, T. Hyeon, *Nat. Mater.* **2004**, *3*, 891.
- 8 X. Hu, J. C. Yu, J. Gong, Q. Li, G. Li, *Adv. Mater.* **2007**, *19*, 2324.
- 9 X. Hu, J. C. Yu, *Adv. Funct. Mater.* **2008**, *18*, 880.
- 10 X. Hu, J. Gong, L. Zhang, J. C. Yu, *Adv. Mater.* **2008**, *20*, 4845.
- 11 L. Lu, A. Eychmuller, *Acc. Chem. Res.* **2008**, *41*, 244.
- 12 JCPDS No. 76-0086, $a = 5.422 \text{ \AA}$ and $c = 8.395 \text{ \AA}$.
- 13 Supporting Information is available electrically on the CSJ-Journal Web site, <http://www.csj.jp/journals/chem-lett/index.html>.